Symmetry breaking in a bull and bear financial market model

Iryna Sushko,[a*] *Fabio Tramontana,*[b], *Frank Westerhoff,*[c] *Viktor Avrutin*[d]

[a]Institute of Mathematics, National Academy of Sciences of Ukraine, 3 Tereshchenkivska st., 01601 Kyiv, Ukraine

[b]Department of Economics and Management, University of Pavia, via S.Felice 5, 27100 Pavia, Italy

[c]Department of Economics, University of Bamberg, Feldkirchenstrasse 21, 96045 Bamberg, Germany

[d]DESP, University of Urbino, via Saffi 42, 61029 Urbino, Italy

Abstract

We investigate bifurcation structures in the parameter space of a one-dimensional piecewise linear map with two discontinuity points. This map describes endogenous bull and bear market dynamics arising from a simple asset-pricing model. An important feature of our model is that some speculators only enter the market if the price is sufficiently distant to its fundamental value. Our analysis starts with the investigation of a particular case in which the map is symmetric with respect to the origin, associated with equal market entry thresholds in the bull and bear market. We then generalize our analysis by exploring how novel bifurcation structures may emerge when the map's symmetry is broken.

1 Introduction

Research in financial market models with interacting chartists and fundamentalists has made considerable progress in recent years. For surveys, see Chiarella *et al.* (2009), Hommes and Wagener (2009), Lux (2009) and Westerhoff (2009). According to these models, the dynamics of financial markets is not caused solely by the arrival of exogenous fundamental shocks, but also depends on the endogenous trading activity of heterogeneous speculators. These models, some of which are able to mimic a number of important stylized facts of financial markets, including bubbles and crashes

*Corresponding author: Institute of Mathematics, National Academy of Sciences of Ukraine, 3 Tereshchenkivska st., 01601 Kyiv, Ukraine, email: sushko@imath.kiev.ua

and excess volatility, clearly help us to gain a better understanding of how financial markets function. The dynamics of these models is usually due to some kind of *non-linearity* which arises from speculators' trading behavior. For instance, in the models of Day and Huang (1990), Chiarella (1992) and Tramontana *et al.* (2009), speculators follow non-linear technical or fundamental trading rules and, as a consequence, complex price dynamics may arise. Non-linearities may also arise if speculators switch between technical and fundamental trading rules, as in the models of Kirman (1991), Brock and Hommes (1998), and Lux and Marchesi (1999), or if they switch between different markets, as in Westerhoff (2004), Chiarella *et al.* (2005, 2007), and Huang and Chen (2014).

Only a few models are represented by *piecewise linear* maps. This is surprising since piecewise linear maps enable very in-depth analytical investigation of dynamic properties of a model. Contributions in this direction include Huang and Day (1993), Day (1997), Tramontana *et al.* (2010), Huang *et al.* (2010) and Huang and Zheng (2012). Recently, we therefore started to consider financial market models in which some speculators are always active in the market while others only become active if mispricing, i.e. the distance between the current price of an asset and its fundamental value, is large enough (see Tramontana *et al.* 2010, 2013, 2014). Assuming that speculators' trading rules are otherwise linear, such a perspective leads to simple models which possess piecewise linear structures. Until now, we have only considered cases in which the threshold value of the misalignment in the bull market is the same as the corresponding threshold value in the bear market. In this way, we obtained a one-dimensional piecewise linear map (1D PWL map for short) with three linear branches and two *symmetric* discontinuity points. In this paper we remove this simplifying assumption by considering a financial market model in which the two threshold values differ.

To be precise, the model considered in the present paper is defined by a 1D PWL map f with three linear branches and two (not necessarily symmetric) discontinuity points. We are interested in the *bifurcation structure* of the map's parameter space. In particular, we study parameter regions called *periodicity regions*, related to attracting cycles of different periods. Obviously, in the presence of two discontinuity points, the bifurcation structure may be much more complicated than those observed in the parameter space of a map with one discontinuity point. In fact, the dynamics of a generic 1D PWL map with one discontinuity point, say, map g, are relatively well understood (see, e.g., Keener 1980, Gardini *et al.* 2010, Gardini *et al.* 2014, and references therein). For instance, there are two basic bifurcation structures for the periodicity regions of map g, namely the period adding structure and the period incrementing structure.

The *period adding structure* is associated with the invertibility of map g on its absorbing interval, in which case map

g can only have attracting cycles and quasiperiodic orbits, but no chaotic attractors. We observe such a bifurcation structure in the parameter space of map g when its linear branches are both increasing functions. The period adding structure is formed by periodicity regions which are ordered in the parameter space according to the Farey summation rule applied to the rotation numbers of the related cycles. For example, between two periodicity regions related to cycles with rotation numbers $1/2$ and $1/3$ there is a region corresponding to cycles with rotation number $2/5$. Similar structures, also called Arnold tongues or mode-locking tongues, are observed in the parameter space of two- and higher-dimensional maps near a Neimark-Sacker bifurcation boundary, in a certain class of circle maps, in 1D PWL continuous bimodal maps, etc. The boundaries of the periodicity regions belonging to the period adding structure are defined by the conditions of *border collision bifurcations* of the related cycle occurring when a point of the cycle collides with a discontinuity point under parameter variation. In contrast, the *period incrementing structure* is much simpler. It is associated with increasing and decreasing branches of map g, and is formed by periodicity regions related to basic cycles, ordered according to increasing periods, with overlapping parts of two neighboring regions and bistability. Recall that a basic cycle has only one point in the left (right) partition of the map while all its other points are located in the right (left) partition of the map.

It is clear that the parameter space of a 1D PWL map with two discontinuity points contains regions, associated with absorbing intervals involving only one discontinuity point, in which case the aforementioned period adding and the period incrementing structures can be observed. However, there are also more complicated bifurcation structures that involve both discontinuity points. In fact, for map f considered in the symmetric case ($z^- = z^+$), studied in Tramontana *et al.* (2013), four bifurcation structures are observed. Two of these can be explained on the basis of standard period adding and period incrementing structures, while two other structures, associated with both discontinuity points, are non-standard. Namely, there is an *even-period incrementing structure* and a particular period adding structure, the explicit description of which was left for future work. In the present paper, we first describe these structures in detail and then break the symmetry of the map by considering that $z^+ = z^- + \varepsilon$ for some small $\varepsilon > 0$, in order to find possible distortions of the aforementioned bifurcation structures. We show that there are parameter regions in which the period adding and period incrementing structures are preserved, being only quantitatively modified. However, new substructures also appear which are related to the two discontinuity points.

Overall, our simple asset-pricing model possesses a surprisingly rich bifurcation structure. Note that the cycles we

study in our paper imply excess volatility, since the fundamental value of the asset is constant. Moreover, the cycles can be located in the bull or bear market, or they can stretch over bull and bear markets. Economically, this means that the model is able to explain periods of persistent misalignments and the emergence of endogenous bubbles and crashes. Without question, the primary goal of our paper is to contribute to the bifurcation theory of 1D PWL maps with two discontinuity points. However, the fact that our analysis also offers valuable insights into the functioning of financial markets should not be overlooked. Bubbles and crashes and excess volatility can have very negative consequences for the real economy. It is therefore crucial for us to understand what drives these two phenomena.

The rest of our paper is organized as follows. In Section 2, we introduce our financial market model. In Section 3, we recap what is known about its bifurcation structure in the symmetric case (i.e. $z^- = z^+$), and consider in more detail a particular period adding structure, associated with two discontinuity points, for which only few preliminary results exist as yet. In Section 4, we explore how the bifurcation structures are modified when the map's symmetry is broken (i.e. $z^- \neq z^+$). Section 5 concludes our paper and identifies a few avenues for future research.

2 A simple piecewise linear financial market model

Our model may be regarded as a generalization of the models of Huang and Day (1993) and Tramontana *et al.* (2013). In a nutshell, the model's structure may be summarized as follows. We assume that there are chartists, fundamentalists and market makers who can trade one risky asset. Chartists bet on the persistence of bull and bear markets while fundamentalists believe in mean reversion. Market makers clear the market and adjust the price of the asset with respect to speculators' excess demand. What makes the model interesting is that there are two types of chartists and fundamentalists: type 1 chartists and type 1 fundamentalists are always active while type 2 chartists and type 2 fundamentalists only enter the market if the asset's mispricing exceeds a certain critical threshold. We present the model's building blocks in Section 2.1 and derive its dynamical system in Section 2.2.

2.1 The setup of the model

Market makers adjust the price of the asset on the basis of a linear price-adjustment rule. Accordingly, they quote the price of the asset for period $t+1$ as

$$P_{t+1} = P_t + a\left(D_t^{C,1} + D_t^{F,1} + D_t^{C,2} + D_t^{F,2}\right). \tag{1}$$

The four terms in the bracket on the right-hand side of (1) capture the orders placed by type 1 chartists, type 1 fundamentalists, type 2 chartists and type 2 fundamentalists, respectively. Moreover, parameter a is a positive price adjustment parameter that determines how strongly market makers adjust the price of the asset with respect to excess demand. Without loss of generality, we set $a = 1$.

Chartists classify a bull (bear) market as a market in which the price of the asset is above (below) its fundamental value. When prices are in the bull (bear) region, chartists optimistically (pessimistically) buy (sell) assets. Let F be the asset's fundamental value. Type 1 chartists are always active, and their orders can be represented as

$$D_t^{C,1} = c_1(P_t - F). \tag{2}$$

Reaction parameter c_1 is positive, and indicates how aggressively type 1 chartists react to their price signals. Type 2 chartists wait for a stronger price signal before they enter the market. Their orders are formalized as

$$D_t^{C,2} = \begin{cases} c_2(P_t - F) + c_3 & for \quad P_t - F \geq z^+, \\ 0 & for \quad -z^- < P_t - F < z^+, \\ c_2(P_t - F) - c_3 & for \quad P_t - F \leq -z^-. \end{cases} \tag{3}$$

Parameters z^+ and z^- are positive, and capture how large the deviation between the current price and its fundamental value must be for type 2 chartists to enter the market in the bull market and bear market, respectively. Reaction parameter $c_2 > 0$ controls the trading intensity of type 2 chartists with respect to their price signals. Parameter c_3 enables type 2 chartists' transactions to be adjusted such that they are non-negative in a bull market and non-positive in a bear market. In this paper, we achieve this by assuming that $c_3 \geq \max[-c_2 z^+; -c_2 z^-]$.

Orders placed by type 1 and type 2 fundamentalists are formulated similarly except for the fact that they buy assets in undervalued markets and sell assets in overvalued markets. Orders placed by type 1 and type 2 fundamentalists are given as

$$D_t^{F,1} = f_1(F - P_t) \tag{4}$$

and

$$D_t^{F,2} = \begin{cases} f_2(F - P_t) - f_3 & for \quad P_t - F \geq z^+, \\ 0 & for \quad -z^- < P_t - F < z^+, \\ f_2(F - P_t) + f_3 & for \quad P_t - F \leq -z^-, \end{cases} \tag{5}$$

respectively. Note that f_1 and f_2 are positive reaction parameters, determining the aggressiveness of type 1 and type 2 fundamentalists, while parameter $f_3 \geq \max[-f_2 z^+; -f_2 z^-]$ ensures that the orders placed by type 2 fundamentalists are non-positive in overvalued markets and non-negative in undervalued markets.

2.2 The model's map and some preliminary remarks

By inserting the four demand functions (2-5) into the price adjustment rule (1), we obtain, after rearranging

$$P_{t+1} = \begin{cases} P_t + (c_1 + c_2 - f_1 - f_2)(P_t - F) + c_3 - f_3 & for \quad P_t - F \geq z^+, \\ P_t + (c_1 - f_1)(P_t - F) & for \quad -z^- < P_t - F < z^+, \\ P_t + (c_1 + c_1 - f_1 - f_2)(P_t - F) - c_3 + f_3 & for \quad P_t - F \leq -z^-. \end{cases} \tag{6}$$

It is convenient to express our model in terms of deviations from the asset's fundamental value by introducing the new variable $x_t = P_t - F$. Moreover, let us simplify the notation by defining $s_1 = c_1 - f_1$, $s_2 = c_2 - f_2$ and $m = c_3 - f_3$. Our model then turns into the following 1D PWL map

$$f : x \to f(x) = \begin{cases} f_R(x) = (1 + s_1 + s_2)x + m & for \quad x \geq z^+, \\ f_M(x) = (1 + s_1)x & for \quad -z^- < x < z^+, \\ f_L(x) = (1 + s_1 + s_2)x - m & for \quad x \leq -z^-. \end{cases} \tag{7}$$

In Tramontana *et al.* (2013), the dynamics of map f is explored for the case $z^+ = z^-$, i.e. for the case in which the market entry thresholds for type 2 chartists and type 2 fundamentalists are symmetrically located around the asset's fundamental value. Moreover, they assume that $s_1 > 0$ so that the slope of $f_M(x)$ is greater than 1. In the present paper, we retain the assumption of $s_1 > 0$, but study how the bifurcation structures in the (m, s_2)-parameter plane change if the symmetry of market entry thresholds is broken. Our focus is on regular dynamics, that is, on bifurcation structures formed by parameter regions called *periodicity regions*, related to attracting cycles of map f.

In order to describe a cycle of map f, it is convenient to use its symbolic representation. To this end, we first associate symbol L with partition $I_L = (-\infty, -z^-)$, M_- with $I_{M_-} = (-z^-, 0)$, M_+ with $I_{M_+} = (0, z^+)$ and R with $I_R = (z^+, \infty)$. Then the symbolic representation of an n-cycle $\{x_i\}_{i=1}^n$, where $x_i \in I_{\sigma_i}$, $\sigma_i \in \{L, M_-, M_+, R\}$, is the *symbolic sequence* $\sigma = \sigma_1 \sigma_2 ... \sigma_n$.

Recall that a boundary of a periodicity region related to an attracting n-cycle of a 1D piecewise linear discontinuous map is defined either by the condition of a *border collision bifurcation* (BCB for short) of the cycle occurring when

a point of the cycle collides with a discontinuity point, or by the condition of a *degenerate flip bifurcation* (DFB) of the cycle associated with its eigenvalue crossing -1, or by the condition of a *degenerate bifurcation associated with its eigenvalue crossing* $+1$ (DB+1). For details concerning degenerate bifurcations, we refer to Sushko and Gardini (2010).

A BCB of an n-cycle of the considered map f occurs if one of the periodic points collides with either $x = -z^-$ or $x = z^+$. Such a periodic point is called the *colliding point*. If a colliding point approaches the discontinuity point $x = -z^-$ or $x = z^+$ from the left, then the BCB condition is $f^{n-1}(f_L(-z^-)) = -z^-$ or $f^{n-1}(f_M(z^+)) = z^+$, respectively. If a colliding point approaches the discontinuity point from the right, then the BCB condition is $f^{n-1}(f_M(-z^-)) = -z^-$ or $f^{n-1}(f_R(z^+)) = z^+$, respectively. Moreover, a BCB condition of an n-cycle can be written as $f_\sigma(z) = z$, where $z \in \{-z^-, z^+\}$ is the related discontinuity point and f_σ denotes a composite function associated with the colliding point: $f_\sigma(x) = f_{\sigma_1} \circ f_{\sigma_2} \circ ... \circ f_{\sigma_n}(x)$ (note that $f_{M_-} = f_{M_+} = f_M$). The limiting values of f at the discontinuity points are called *critical points* and denoted as follows:

$$\begin{aligned} c_L^- &= f_L(-z^-), \quad c_M^- = f_M(-z^-), \\ c_M^+ &= f_M(z^+), \quad c_R^+ = f_R(z^+). \end{aligned}$$

3 Symmetric case

Let us first recall what is known about the bifurcation structure of the parameter space of map f in the case of symmetric market entry thresholds $z^+ = z^- = z$ (see Tramontana *et al.* (2013) for details). After a suitable rescaling of x, map f can, in the symmetric case, be written as follows:

$$f_s : x \to f_s(x) = \begin{cases} f_L(x) = (1 + s_1 + s_2)x - m & for \quad x \leq -1, \\ f_M(x) = (1 + s_1)x & for \quad -1 < x < 1, \\ f_R(x) = (1 + s_1 + s_2)x + m & for \quad x \geq 1. \end{cases} \tag{8}$$

A 2D bifurcation diagram of map f_s in the (m, s_2)-parameter plane is shown in Fig. 1. Here, the dark gray regions are related to divergence of a generic orbit; white regions are related to chaotic attractors; colored regions are associated with attracting cycles of different periods where the correspondence of colors and periods is given in the color bar; and, the overlapping parts of some neighboring regions are light gray. Note that one of the characteristic features of map f_s is its symmetry with respect to the origin, which leads to a simple conclusion being drawn: any invariant set A of f is either symmetric with respect to the origin, or there exists another invariant set A' which is symmetric to A. In

particular, an odd period cycle necessarily coexists with a symmetric cycle, while an even period cycle, if it is symmetric, may be unique. Domains R_i, $i = \overline{1,4}$, indicated in Fig. $1a$, are distinguished according to the sign of offset m and the sign of the slope of the outermost branches $(1 + s_1 + s_2)$:

$$R_1 = \{p : s_1 > 0,\ 1 + s_1 + s_2 > 0, m > 0\},\quad R_2 = \{p : s_1 > 0,\ 1 + s_1 + s_2 < 0, m > 0\},$$

$$R_3 = \{p : s_1 > 0,\ 1 + s_1 + s_2 > 0, m < 0\},\quad R_4 = \{p : s_1 > 0,\ 1 + s_1 + s_2 < 0, m < 0\},$$

where p denotes a point in the parameter space of map f_s. Note that for $s_1 = 0.5$ the equality $1 + s_1 + s_2 = 0$ holds for $s_2 = -1.5$.

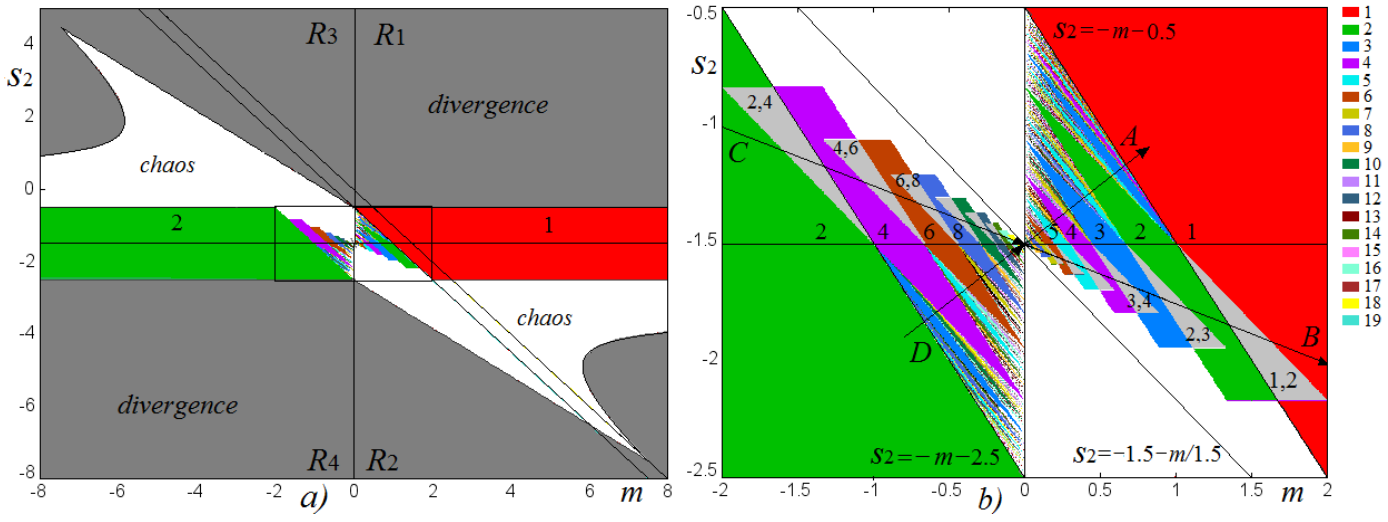

Figure 1: *a)* A 2D bifurcation diagram of map f_s given in (8) in the (m, s_2)-parameter plane for $s_1 = 0.5$; *b)* An enlargement of the window indicated in *a)*. 1D bifurcation diagrams related to parameter paths along the arrows marked A, B, C and D are shown in Figs. $2a$, $2b$, $3a$ and $3b$, respectively.

3.1 Bifurcation structure of domains R_1 and R_2

As shown in Tramontana *et al.* (2013), in domain R_1 for $s_2 < -(m + s_1)$, periodicity regions are organized according to the *period adding structure*. Moreover, each periodicity region is related to two coexisting attracting cycles which are symmetric to each other with respect to the origin. Here the equality $s_2 = -(m + s_1)$ defines the BCB boundary of the region related to the coexisting attracting fixed points R and L. This structure is illustrated in Fig. $2a$ by a 1D bifurcation diagram related to the parameter path indicated by arrow A in Fig. $1b$.

In fact, for the considered parameter region, map f_s has two disjoint (symmetric to each other) absorbing intervals bounded by the related critical points, $I_- = [c_M^-, c_L^-]$ and $I_+ = [c_R^+, c_M^+]$, on each of which the map is invertible and defined by two increasing functions. It is known (see e.g., Gardini *et al.* (2014)) that for this class of maps (also called *gap maps*) the periodicity regions are organized in the period adding structure. Fig. 2*a* reveals two such structures: one of them is associated with discontinuity point $x = -1$, and the symbolic sequences of related cycles contain the symbols L and M_- only (highlighted red in Fig. 2*a*). In particular, cycles of *complexity level one* (also called basic cycles) form two families,

$$\Sigma_{1,1}^- = \left\{LM_-^n\right\}_{n\geq 1}, \quad \Sigma_{1,2}^- = \left\{M_-L^n\right\}_{n\geq 1}.$$

The second period adding structure (highlighted blue in Fig. 2*a*) is associated with discontinuity point $x = 1$ and the symbols M_+, R, where cycles of complexity level one form the following families:

$$\Sigma_{1,1}^+ = \left\{RM_+^n\right\}_{n\geq 1}, \quad \Sigma_{1,1}^+ = \left\{M_+R^n\right\}_{n\geq 1}.$$

Symbolic sequences of *complexity level two* are obtained using consecutive concatenations starting from two neighboring sequences of complexity level one, leading to 2^2 families:

$$\begin{aligned}
\Sigma_{2,1}^- &= \left\{(LM_-^n)^m LM_-^{n+1}\right\}_{n,m\geq 1}, \quad \Sigma_{2,2}^- = \left\{LM_-^n(LM_-^{n+1})^m\right\}_{n,m\geq 1}, \\
\Sigma_{2,3}^- &= \left\{(M_-L^n)^m M_-L^{n+1}\right\}_{n,m\geq 1}, \quad \Sigma_{2,4}^- = \left\{M_-L^n(M_-L^{n+1})^m\right\}_{n,m\geq 1}.
\end{aligned}$$

In order to obtain 2^K families of complexity level $K \geq 3$, similar concatenation procedures can be applied to sequences of families of complexity level $K-1$ (see Leonov (1959), Leonov (1962), Gardini *et al.* (2014)). Another way to determine all families of the period adding structure is to apply the *map replacement technique,* as described in Avrutin *et al.* (2010), and Gardini *et al.* (2010). This method also helps to simplify the calculation procedure for expressions of the boundaries of related periodicity regions.

Families $\Sigma_{2,i}^+$, $i = \overline{1,4}$, of complexity level two related to the second period adding structure are obviously obtained by substituting R instead of L, and M_+ instead of M_- in families $\Sigma_{2,i}^-$ related to the first period adding structure. Families of higher complexity levels are obtained in the same way.

Let σ' denote the symbolic sequence obtained from σ by interchanging R and L, as well as M_+ and M_-. Sequence σ' of the cycle symmetric (with respect to the origin) to the cycle of symbolic sequence σ. Let P_σ denote the periodicity region corresponding to the attracting cycle with symbolic sequence σ.

If one compares periodicity regions P_σ and $P_{\sigma'}$, related to symmetric cycles (and, thus, associated with the two aforementioned period adding structures) then, due to the symmetry of the map, these periodicity regions have the same boundaries. That is, in domain R_1 we observe just one period adding structure associated with coexisting symmetric cycles. Consider, for example, a cycle with symbolic sequence σ containing the symbols M_+ and R. One of the BCB boundaries of periodicity region P_σ is obtained from $f_\sigma(z^+) = z^+$, where σ is the symbolic sequence associated with the colliding periodic point. For map f_s, it holds that $f_R(x) = -f_L(-x)$, $f_{M_+}(x) = -f_{M_-}(-x)$, thus, $f_\sigma(x) = -f_{\sigma'}(-x)$, so that from $f_\sigma(z^+) = z^+$ we get $-f_{\sigma'}(-z^+) = z^+$, and, finally, $f_{\sigma'}(-z^-) = -z^-$, which corresponds to the condition of the BCB boundary of $P_{\sigma'}$. That is, conditions $f_\sigma(z^+) = z^+$ and $f_{\sigma'}(-z^-) = -z^-$ are equivalent in terms of parameters. For example, the two BCB boundaries of region $P_{RM_+^n}$, $n \geq 1$, related to the basic cycle RM_+^n, are obtained from

$$f_R \circ f_{M_+}^n(z^+) = z^+, \tag{9}$$

$$f_{M_+} \circ f_R \circ f_{M_+}^{n-1}(z^+) = z^+. \tag{10}$$

The conditions defining the BCB boundaries of $P_{LM_-^n}$ are obviously the same up to substitution R by L, M_+ by M_- and z^+ by $-z^-$. Hence we can use the unique notation $P_{LM_-^n,\ RM_+^n}$ for the related region. Similarly, we use the notation $P_{\sigma,\ \sigma'}$ for a generic region of the period adding structure corresponding to two symmetric cycles. It is obvious that if the symmetry $z^- = z^+$ is broken, then periodicity regions of two period adding structures will no longer have the same boundaries, as we will discuss in the next section. In fact, for $z^+ \neq z^-$ the BCB conditions $f_L \circ f_{M_-}^n(-z^-) = -z^-$ and $f_{M_-} \circ f_L \circ f_{M_-}^{n-1}(-z^-) = -z^-$ become different to those given in (9) and (10), and the same occurs for cycles of all other complexity levels.

Note that for $m = 0$, $0 < (1 + s_1 + s_2) < 1$, corresponding to segment $\{(m, s_2) : m = 0, -1.5 < s_2 < -0.5\}$ in Fig. 1, map f_s is topologically conjugate on both absorbing intervals I_- and I_+ to a *circle map* on which a linear rotation with a rational or irrational rotation number is defined. Any point of this segment related to a rational rotation is an issue point of the corresponding periodicity region.

Periodicity regions in domain R_2 are organized in a *period incrementing structure*. It is illustrated by the 1D bifurcation diagram presented in Fig. 2*b* which is related to the parameter path indicated by arrow B in Fig. 1*b*. It can be shown that if $m > -(1 + s_1 + s_2)(1 + s_1)$ (in Fig. 1*b* the related region is defined by $s_2 > -1.5 - m/1.5$), map f_s has two disjoint (symmetric to each other) absorbing intervals, $I_- = [c_M^-, f_L(c_M^-)]$ and $I_+ = [f_R(c_M^+), c_M^+]$, on both of which the map is defined by increasing and decreasing functions. It is known that such a map is characterized (in

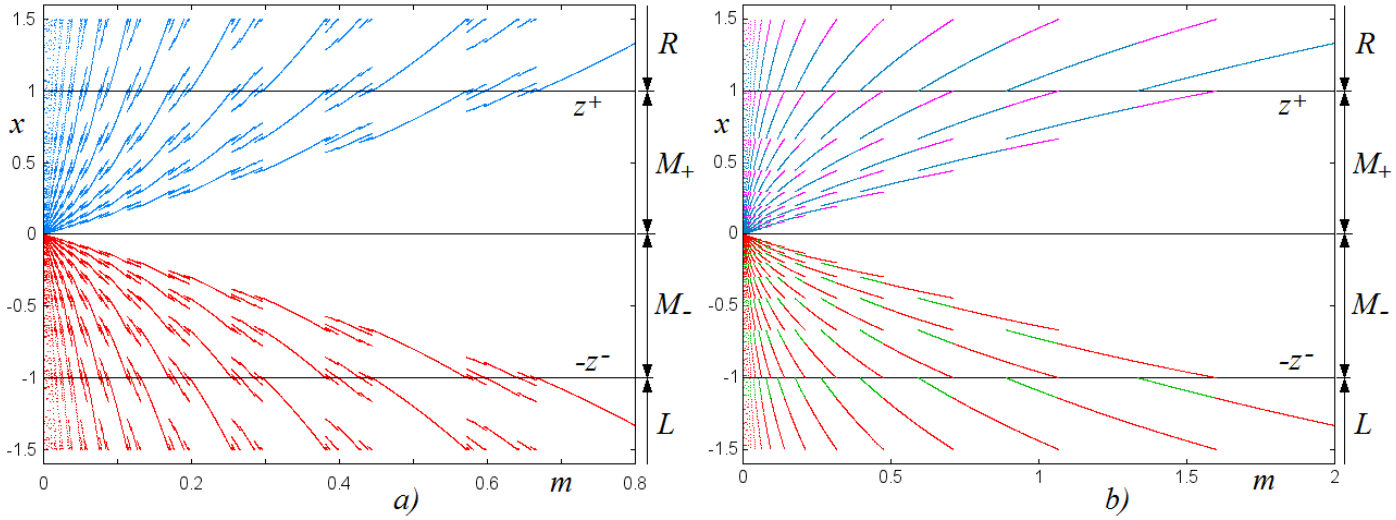

Figure 2: 1D bifurcation diagrams of map f_s given in (8) illustrating in *a)* two coexisting period adding structures, and in *b)* period incrementing structures. Here $s_1 = 0.5$ and in *a)* $s_2 = 0.5m - 1.5$, $0 < m < 0.8$ (see path marked A in Fig. 1*b*), while in *b)* $s_2 = -0.25m - 1.5$, $0 < m < 2$ (see path marked B in Fig. 1*b*).

the stability regime) by period incrementing structures formed by periodicity regions related to the basic cycles, with overlapping parts of each two neighboring regions. As illustrated in Fig. 2*b*, there are two such structures. The first (highlighted red and green), associated with discontinuity point $x = -1$, is formed by the periodicity regions $P_{LM_-^n}$ related to basic cycles, with overlapping parts of each two neighboring regions, $P_{LM_-^n}$ and $P_{LM_-^{n+1}}$, which correspond to coexisting cycles LM_-^n and LM_-^{n+1}. The second period incrementing structure (highlighted blue and magenta in Fig. 2*b*) is associated with discontinuity point $x = 1$, and is formed by the periodicity regions $P_{RM_+^n}$ of basic cycles, with overlapping parts of each two neighboring regions.

As already discussed, the symmetry of the map with respect to zero leads to the fact that the BCB boundaries of $P_{LM_-^n}$ and $P_{RM_+^n}$ coincide in the parameter space, meaning that we see just one period incrementing structure in domain R_2, and each region of this structure is denoted by $P_{LM_-^n,\ RM_+^n}$. In contrast to the periodicity regions of the period adding structure, having only BCB boundaries, any region $P_{LM_-^n,\ RM_+^n}$ of the period incrementing structure also has a DFB boundary defined by

$$(1 + s_1 + s_2)(1 + s_1)^{n-1} = -1$$

(obviously, the DFB boundaries of $P_{LM_-^n}$ and $P_{RM_+^n}$ coincide as well). Hence, each region $P_{LM_-^n,\ RM_+^n}$ is related to

two coexisting cycles, LM_-^n and RM_+^n, while its part that overlaps with neighboring region $P_{LM_-^{n+1},\ RM_+^{n+1}}$ is related to four coexisting cycles, LM_-^n, LM_-^{n+1}, RM_+^n and RM_+^{n+1}. Obviously, if the symmetry $z^- = z^+$ is broken, then the BCB boundaries of periodicity regions of the two period incrementing structures become different.

Note that at the border between domains R_1 and R_2 defined by $(1+s_1+s_2)=0$, periodicity regions are organized in period incrementing structure without overlapping, and each region corresponds to coexisting superstable basic cycles LM_-^n and RM_+^n, $n \geq 0$.

3.2 Bifurcation structure of domains R_3 and R_4

As we have seen, the period adding structure in domain R_1 and the period incrementing structure in domain R_2 are well known. The basic mechanisms of their formation can be described using symbolic sequences consisting of two symbols only. The bifurcation structures observed in domains R_3 and R_4 are associated with four symbols; such structures have been studied to a much lesser extent (see, e.g., Tramontana *et al.* (2012), Tramontana *et al.* (2015)).

Let us recall first how the periodicity regions in domain R_3 are organized. Fig. 3*a* shows the 1D bifurcation diagram corresponding to the parameter path indicated by arrow C in Fig. 1*b*. As shown in Tramontana *et al.* (2013), periodicity regions in this domain are organized in an *even-period incrementing structure* formed by regions $P_{LM_+^nRM_-^n}$, $n \geq 0$, related to the cycle of even period $2(n+1)$, with overlapping parts of each two neighboring regions corresponding to coexisting cycles $LM_+^nRM_-^n$ and $LM_+^{n+1}RM_-^{n+1}$.

In fact, in domain R_3 for $m < -(1+s_1+s_2)(1+s_1)$ (in Fig. 1*b* this condition corresponds to $s_2 < -1.5 - m/1.5$), map f_s has an invariant absorbing set consisting of two intervals: $I = \left[c_M^-, f_R(c_M^+)\right] \cup \left[f_L(c_M^-), c_M^+\right]$. The condition $m < -(1+s_1+s_2)(1+s_1)$ is obtained from the condition $f_R(c_M^+) < 0$ or, equivalently, $f_L(c_M^-) > 0$, in which case the two intervals mentioned above are disjoint. Two BCB boundaries of the periodicity region $P_{LM_+^nRM_-^n}$, $n \geq 1$, are obtained from

$$f_R \circ f_{M_-}^n \circ f_L \circ f_{M_+}^n(z^+) = z^+ \tag{11}$$

(or, equivalently, $f_L \circ f_{M_+}^n \circ f_R \circ f_{M_-}^n(-z^-) = -z^-$) and

$$f_{M_+} \circ f_R \circ f_{M_-}^n \circ f_L \circ f_{M_+}^{n-1}(z^+) = z^+ \tag{12}$$

(or equivalently, $f_{M_-} \circ f_L \circ f_{M_+}^n \circ f_R \circ f_{M_-}^{n-1}(-z^-) = -z^-$), while the DB+1 boundary is defined by

$$(1+s_1+s_2)(1+s_1)^n = 1.$$

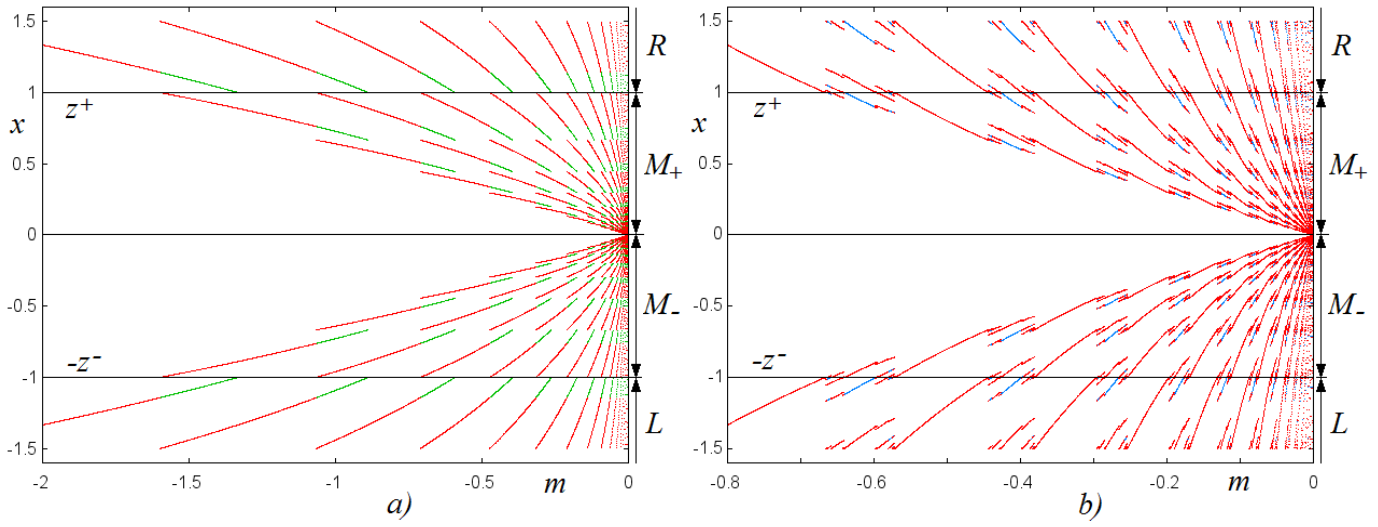

Figure 3: 1D bifurcation diagrams of map f_s given in (8) illustrating in *a)* an even-period incrementing structure and in *b)* a period adding structure, with coexisting cycles of odd periods. Here $s_1 = 0.5$ and in *a)* $s_2 = -0.25m - 1.5$, $-2 < m < 0$ (see path marked C in Fig. 1*b*), while in *b)* $s_2 = 0.5m - 1.5$, $-0.8 < m < 0$ (see path marked D in Fig. 1*b*).

(Obviously, when the symmetry $z^+ = z^-$ is broken, the conditions associated with z^- are no longer equivalent to those given in (11) and (12).) Periodicity region P_{LR} is bounded by the BCB boundary obtained from $f_R \circ f_L(z^+) = z^+$ (or, equivalently, $f_L \circ f_R(-z^-) = -z^-$), that holds for $s_2 = -m - 2 - s_1$ or for $s_2 = -s_1$ (i.e. $s_2 = -m - 2.5$ and $s_2 = -0.5$ in Fig. 1), and the DB+1 boundary defined by $(1 + s_1 + s_2) = 1$, that is, $s_2 = -s_1$. Note that region P_{LR} also extends to domain R_4, where it has one more stability boundary, related to the DFB of cycle LR, defined by $(1 + s_1 + s_2) = -1$, that is, $s_2 = -2 - s_1$ (in Fig. 1 this boundary is given by $s_2 = -2.5$).

Comparing the period incrementing structure in domain R_2 with that in R_3 (see Fig. 1*b*; cf also Fig. 2*b* and Fig. 3*a*), one can note the symmetry of these structures with respect to the parameter point

$$S = (m, s_2) = (0, -(1 + s_1)) \tag{13}$$

associated with $f_L(x) = f_R(x) \equiv 0$. However, the symmetric parameter regions are related to different cycles, namely, region $P_{LM_-^n,\, RM_+^n} \subset R_2$, $n \geq 0$, is symmetric with respect to S to region $P_{LM_+^n RM_-^n} \subset R_3$. To prove this, recall that one BCB boundary of $P_{LM_-^n,\, RM_+^n} \subset R_2$ is defined by the condition $f_R \circ f_{M_+}^n(z^+) = z^+$, moreover, the condition $f_L \circ f_{M_-}^n(-z^-) = -z^-$ also holds. Let parameter point $p^* = (m^*, s_2^*) \in R_2$ satisfy the condition $f_R \circ f_{M_+}^n(z^+) = z^+$.

Then it is easy to show that at parameter point $p' = (-m^*, -2(1+s_1) - s_2^*) \in R_3$, which is symmetric to p^* with respect to S, it holds that $f_R \circ f_{M_-}^n(z^+) = -z^-$ and $f_L \circ f_{M_-}^n(-z^-) = z^+$. Therefore, parameter point p' satisfies the condition $f_R \circ f_{M_-}^n \circ f_L \circ f_{M_+}^n(z^+) = z^+$, which is related to the BCB boundary of $P_{LM_+^n RM_-^n} \subset R_3$. Similarly, it can be shown that the second BCB boundary of $P_{LM_-^n,\ RM_+^n} \subset R_2$ is symmetric to the second BCB boundary of $P_{LM_+^n RM_-^n} \subset R_3$. Finally, the DFB boundary of $P_{LM_-^n,\ RM_+^n}$ is obviously symmetric with respect to S to the DB+1 boundary of $P_{LM_+^n RM_-^n}$.

Now let us consider the bifurcation structure of domain R_4, illustrated in Fig. 3*b* by the 1D bifurcation diagram corresponding to parameter path D shown in Fig. 1*b*. One can see a particular period adding structure where any odd period cycle coexists with the symmetric (with respect to the origin) cycle, while any even period cycle is a unique attractor, being symmetric itself. Tramontana *et al.* (2013) left an explicit description of this structure for future work, hence it is discussed below in more detail.

In fact, in domain R_4 map f_s has an invariant absorbing set consisting of two symmetric intervals, $I = \left[c_M^-, c_R^+\right] \cup \left[c_L^-, c_M^+\right]$. The condition $f_M(c_R^+) < f_R(c_M^+)$, as well as $f_M(c_L^-) > f_L(c_M^-)$, equivalent to $ms_1 < 0$, obviously holds in R_4, thus, f_s is a gap map on I (that is, it is invertible in I), which is known to be unable to have chaotic attractors, but only attracting cycles and quasiperiodic orbits (so-called Cantor set attractors). Similar to the case of the period adding structure observed in domain R_1, the period adding structure in R_4 originates from the straight line with $m = 0$, namely, from its segment with $-2 - s_1 < s_2 < -1 - s_1$ (in Fig. 1*b* it corresponds to the segment $\{(m, s_2) : m = 0,\ -2.5 < s_2 < -1.5\}$), at which the condition $f_M(c_R^+) = f_R(c_M^+)$ holds (as well as $f_M(c_L^-) = f_L(c_M^-)$). For parameter values belonging to this segment, map f_s is topologically conjugate to a circle map with a rational or irrational rotation number. Each point of the segment related to rational rotation is an issue point of the related periodicity region in R_4. For example, point $(m, s_2) \approx (0, -2.3165)$ is an issue point of the periodicity region related to cycles with rotation number 1/3 (see Fig. 4*a*), or point $(m, s_2) \approx (0, -2.1662)$ is an issue point of the periodicity region corresponding to cycles with rotation number 1/4 (see Fig. 5*a*). If a parameter point enters a periodicity region related to an odd period cycle, then two symmetric cycles of this period are born, as shown, for example, in Fig. 4*b*. Obviously, due to the symmetry of f_s, BCBs of these cycles occur at the same parameter values, which is why we observe just one periodicity region for each pair of odd period cycles. If a parameter point enters a periodicity region related to even period, then only one cycle of this period is born, which itself is symmetric with respect to the origin (see, e.g., Fig. 5*b*).

In order to obtain the symbolic sequences of the cycles of f_s associated with the period adding structure in domain

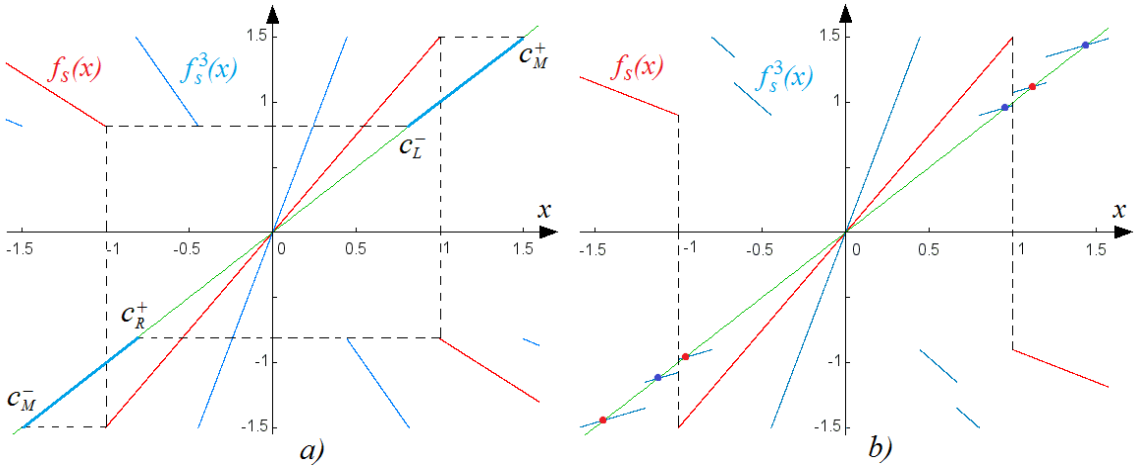

Figure 4: *a)* Map f_s and f_s^3 for $s_1 = 0.5$, $s_2 = -2.3165$, $m = 0$, when any point of $I = [c_M^-, c_R^+] \cup [c_L^-, c_M^+]$ is 3-periodic; *b)* f_s, f_s^3 and two coexisting 3-cycles for $s_1 = 0.5$, $s_2 = -2$, $m = -0.4$.

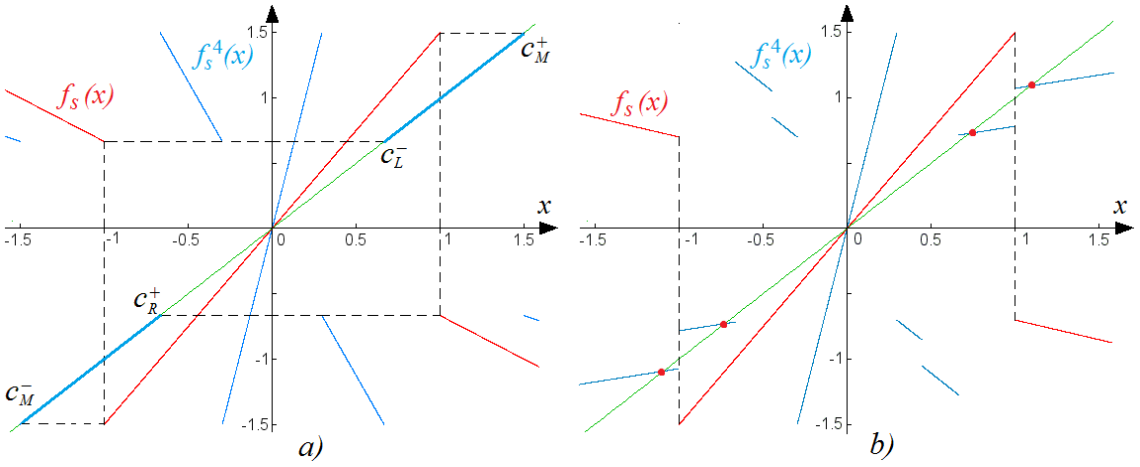

Figure 5: *a)* Map f_s and f_s^4 for $s_1 = 0.5$, $s_2 = -2.1662$, $m = 0$, when any point of $I = [c_M^-, c_R^+] \cup [c_L^-, c_M^+]$ is 4-periodic; *b)* f_s, f_s^4 and attracting 4-cycle for $s_1 = 0.5$, $s_2 = -1.8$, $m = -0.4$.

R_4, first note that there is a rule to check the admissibility of such symbolic sequences: it is easy to see that a point $x_0 \in I_L$ ($x_0 \in I_R$) is mapped in *one* iteration either to a point $x_1 \in I_R$ ($x_1 \in I_L$) or $x_1 \in I_{M_+}$ ($x_1 \in I_{M_-}$), while a point $x_0 \in I_{M_+}$ ($x_0 \in I_{M_-}$) is mapped either to a point $x_1 \in I_{M_+}$ ($x_1 \in I_{M_-}$), or $x_1 \in I_R$ ($x_1 \in I_L$) (see, for example, Fig. 5). That is, in a symbolic sequence σ, symbol L (R) is necessarily followed by R or M_+ (L or M_-), while M_+ (M_-) is followed by M_+ or R (M_- or L).

Similar to the symmetry of the period incrementing structures in R_2 and R_3 with respect to parameter point S given

in (13), there is a symmetry of the period adding structure in domain R_1 with that in R_4 (see Fig. 6; cf also Figs. 2*a* and 3*b*). However, it can be seen that these structures are related to cycles with different symbolic sequences; the periods may also differ. The simplest example is region $P_{L,R} \subset R_1$, which is symmetric with respect to point S to region $P_{LR} \subset R_4$: it is easy to check that all the boundaries of $P_{L,R}$ are symmetric with respect to S to the corresponding boundaries of P_{LR} .

Consider first the region $P_{LM_-^n,\ RM_+^n} \subset R_1$, $n \geq 1$, corresponding to the coexisting basic $(n+1)$-cycles LM_-^n and RM_+^n. In order to show that this region is symmetric with respect to S to the region $P_{LM_+^nRM_-^n} \subset R_4$, similar arguments can be used as those related to the symmetry of regions $P_{LM_-^n,\ RM_+^n} \subset R_2$ and $P_{LM_+^nRM_-^n} \subset R_3$. The symbolic sequences $LM_+^nRM_-^n$ are obviously admissible, and, in fact, they are associated with the greatest periodicity regions visible in Fig. 6*b*, such as regions $P_{LM_+RM_-}$, $P_{LM_+^2RM_-^2}$, $P_{LM_+^3RM_-^3}$, etc., which extend, with overlapping parts, also to domain R_3. See also cycles LM_+RM_- and $LM_+^2RM_-^2$, indicated in Fig. 7.

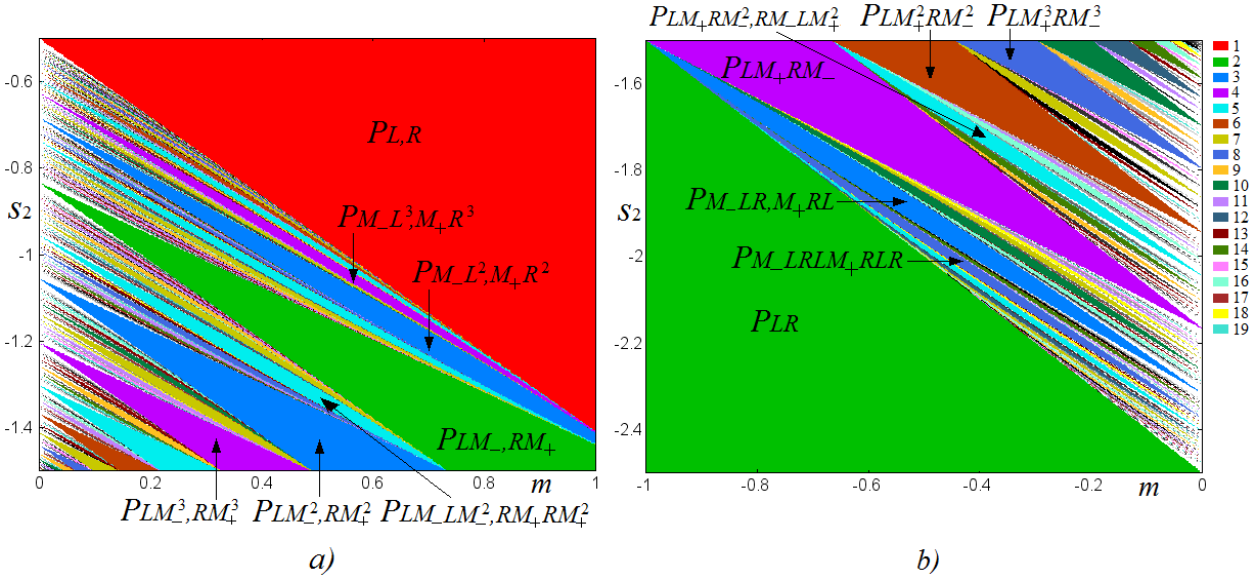

Figure 6: The period adding structure of map f_s for $s_1 = 0.5$ in domain R_1 *a)* and in domain R_4 *b)*.

Now let us consider regions $P_{M_-L^n,\ M_+R^n} \subset R_1$, $n \geq 1$, related to the coexisting basic cycles M_-L^n and M_+R^n. These regions are located in R_1 between region $P_{L,R}$ and region $P_{LM_-,\ RM_+}$ (see Fig. 6*a*). Periodicity regions in R_4 symmetric to $P_{M_-L^n,\ M_+R^n}$ are located between regions P_{LR} and $P_{LM_+RM_-}$ (see Fig. 6*b*). In order to obtain a correspondence of cycles M_-L^n, M_+R^n existing for $p \in P_{M_-L^n,\ M_+R^n} \subset R_1$ and those existing for the symmetric (with respect to S) parameter point $p' \in P' \subset R_4$, we can use one more rule: it is easy to check that, due to the symmetry of f_s,

it holds that $f_L \circ f_L(x)|_{x \in I_L,\ p \in P_{M_-L^n,\ M_+R^n}} = f_R \circ f_L(x)|_{x \in I_L,\ p' \in P'}$, and $f_R \circ f_R(x)|_{x \in I_R,\ p \in P_{M_-L^n,\ M_+R^n}} = f_L \circ f_R(x)|_{x \in I_R,\ p' \in P'}$. Hence, if one takes a parameter point $p \in P_{M_-L^n,\ M_+R^n}$ where $n \geq 2$ is *even* (that is, at p the number of applications of f_L or f_R is even), then point p' is related to two coexisting $(n+1)$-cycles $M_-(LR)^{n/2}$ and $M_+(RL)^{n/2}$. That is, region $P_{M_-L^n,\ M_+R^n} \subset R_1$ for even $n \geq 2$ is symmetric to region $P' = P_{M_-(LR)^{n/2},\ M_+(RL)^{n/2}} \subset R_4$. As an example, one can compare the region $P_{M_-L^2,\ M_+R^2} \subset R_1$, indicated in Fig. 6*a*, with the region $P_{M_-LR,\ M_+RL} \subset R_4$ symmetric to it, indicated in Fig. 6*b* (see also Fig. 7 where cycles $M_-LR,\ M_+RL$ are visible). In the meantime, if $p \in P_{M_-L^n,\ M_+R^n}$ where $n \geq 1$ is *odd* (that is, the number of applications of f_L or f_R is odd), then the symmetric point $p' \in P' \subset R_4$ is related to one $2(n+1)$-cycle $M_-(LR)^{(n-1)/2} LM_+(RL)^{(n-1)/2} R$. That is, region $P_{M_-L^n,\ M_+R^n} \subset R_1$ for odd $n \geq 1$ is symmetric to region $P_{M_-(LR)^{(n-1)/2}LM_+(RL)^{(n-1)//2}R} \subset R_4$. One can compare, for example, region $P_{M_-L^3,\ M_+R^3} \subset R_1$ in Fig. 6*a* and region $P_{M_-LRLM_+RLR} \subset R_4$ in Fig. 6*b* (see also Fig. 7 where cycle M_-LRLM_+RLR is shown).

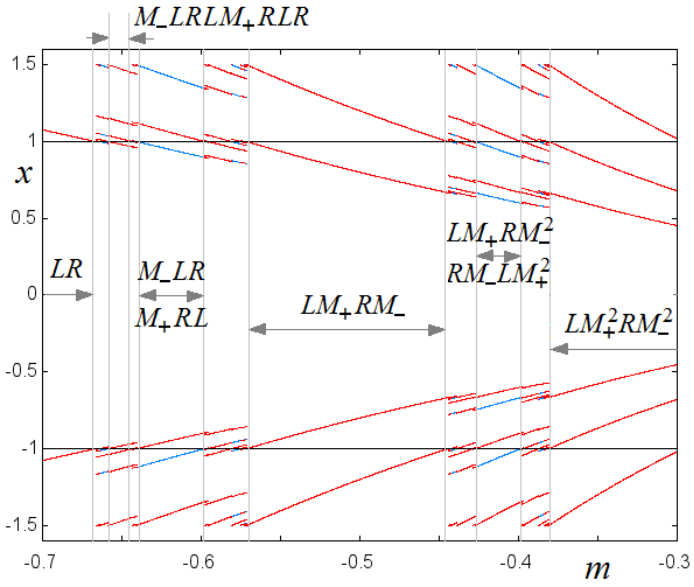

Figure 7: An enlargement of the 1D bifurcation diagram shown in Fig. 3*b*.

Now let us consider region $P_{LM_-^nLM_-^{n+1},\ RM_+^nRM_+^{n+1}} \subset R_1$, $n \geq 1$, associated with two coexisting cycles of complexity level two. Such regions are located between regions $P_{LM_-^n\ ,\ RM_+^n}$ and $P_{LM_-^{n+1}\ ,\ RM_+^{n+1}}$. The periodicity region $P' \subset R_4$ symmetric to $P_{LM_-^nLM_-^{n+1},\ RM_+^nRM_+^{n+1}} \subset R_1$ with respect to S is located between regions $P_{LM_+^nRM_-^n}$ and $P_{LM_+^{n+1}RM_-^{n+1}}$. It can be shown that $P' = P_{LM_+^nRM_-^{n+1},\ RM_-^nLM_+^{n+1}} \subset R_4$, $n \geq 0$. Compare, for example, region $P_{LM_-LM_-^2,\ RM_+RM_+^2} \subset R_1$ indicated in Fig. 6*a* with region $P_{LM_+RM_-^2,\ RM_-LM_+^2} \subset R_4$ shown in Fig. 6*b* (see also the coexisting cycles

$LM_+RM_-^2$, $RM_-LM_+^2$ visible in Fig. 7).

Hence, for the period adding structure observed in domain R_4, we obtain the following families of complexity level one related to cycles with one point in I_L and another in I_R :

$$\left\{LM_+^nRM_-^n\right\},\ \left\{LM_+^nRM_-^{n+1},\ RM_-^nLM_+^{n+1}\right\},\ \text{for } n \geq 0,$$

as well as the following first complexity level families related to cycles with one point in M_- and another in M_+ :

$$\begin{aligned} \left\{M_-\left(LR\right)^{n/2},\ M_+\left(RL\right)^{n/2}\right\},\ \text{for even } n &\geq 2, \\ \left\{M_-\left(LR\right)^{(n-1)/2}LM_+\left(RL\right)^{(n-1)/2}R\right\},\ \text{for odd } n &\geq 1. \end{aligned}$$

The correspondence of other periodicity regions in R_4 with the symmetric one in R_1 can be described similarly. However, it is clear that a generic procedure to obtain symbolic sequences of all complexity levels is more complicated than in the case of a period adding structure based on two symbols.

4 Symmetry breaking

Let us now study how the bifurcation structures of domains R_i, $i = \overline{1,4}$, described in the previous section, change when the equality $z^- = z^+$ in the definition of map f given in (7) does not hold, that is, when the map is no longer symmetric with respect to the origin. To this end, let us consider map f and assume that $z^- = 1$, $z^+ = 1 + \varepsilon$, for some $\varepsilon > 0$. As we shall see, it is rather easy to explain how the period adding and period incrementing structures in domains R_1 and R_2, respectively, are modified because disjoint absorbing intervals, each of which includes only one discontinuity point, persist for such parameter regions. Obviously, qualitatively similar structures are observed for $\varepsilon < 0$ as well (note that to have $z^+ > 0$, it must hold $\varepsilon > -1$). By contrast, the distortion of bifurcation structures of domains R_3 and R_4 is more complicated given that both discontinuity points are involved into absorbing intervals.

4.1 Distortion of bifurcation structures in domains R_1 and R_2

Consider first how the period adding structure in R_1 is modified if $z^- < z^+$. In this case, similar to the symmetric case $z^- = z^+$, map f has two disjoint absorbing intervals, $I_- = [c_M^-, c_L^-]$ and $I_+ = [c_R^+, c_M^+]$, and there are two period adding structures associated with these two intervals. However, now the BCB boundaries of the related periodicity regions no longer coincide, and two coexisting cycles may have different periods.

The bifurcation structure in R_1 is illustrated in Fig. 8 for $z^- = 1$, $z^+ = 1.2$. Fig. 8a shows gray n-periodicity regions, $n = \overline{1,5}$, of the period adding structure related to discontinuity point $x = -z^- = -1$. Let for each cycle associated with periodicity region P_σ the symbolic sequence $\sigma_- \ / \ \sigma_+$ (consisting of the symbols L and M_-) be associated with the periodic point colliding with discontinuity point $x = -1$ from the left/right. Then one BCB boundary of P_σ is related to the condition $f_{\sigma_-}(-z^-) = -z^-$ (these boundaries are colored red in Fig. 8a), and the second BCB boundary of P_σ is related to the condition $f_{\sigma_+}(-z^-) = -z^-$ (these boundaries are colored green in Fig. 8a). The complete period adding structure associated with $x = -1$ is obviously the same as that observed in domain R_1 in the symmetric case (see Fig. 1b or Fig. 6a). As for the period adding structure associated with discontinuity point $x = z^+ = 1.2$, in Fig. 8a the related n-periodicity regions are not colored, while their boundaries related to condition $f_{\sigma'_+}(z^+) = z^+$ are colored blue, and those related to the condition $f_{\sigma'_+}(z^+) = z^+$ are given in magenta. Here, for each cycle related to periodicity region $P_{\sigma'}$, the symbol $\sigma'_+ \ / \ \sigma'_-$ (consisting of symbols R and M_+) is associated with the periodic point colliding with discontinuity point $x = 1.2$ from the right/left. It is easy to show that periodicity region $P_{\sigma'}$ of this period adding structure issues from the same point of the line $m = 0$ as region P_σ (recall that σ' is obtained from σ substituting L with R and M_- with M_+). However, the overall period adding structure is expanded with respect to the first structure.

The two period adding structures can be compared by means of the 1D bifurcation diagram shown in Fig. 8b. For example, for the values of m indicated by gray arrows (see also a segment bounded by points A and B in Fig. 8a) attracting fixed point L (to which any initial point $x_0 < 0$ is attracted) coexists with the cycles colored blue (to which any initial point $x_0 > 0$ is attracted).

The distortion of the period incrementing structure in domain R_2 is illustrated in Fig. 9 for $z^- = 1$ and $z^+ = 1.1$. It is easy to see that for $m > -(1 + s_1 + s_2)(1 + s_1)z^+$ (in Fig. 9a the related region is defined by $s_2 > -1.5 - m/1.5z^+$) map f has two disjoint absorbing intervals, $I_- = [c_M^-, f_L(c_M^-)]$ and $I_+ = [f_R(c_M^+), c_M^+]$, on each of which the map is defined by increasing and decreasing functions. Thus, two period incrementing structures can be observed, associated with these intervals. Obviously, the period incrementing structure related to discontinuity point $x = -z^- = -1$ is the same as in the symmetric case described in the previous section (see Fig. 1b). In Fig. 9a periodicity regions $P_{LM_-^n}$, $n = \overline{0,4}$, belonging to this structure, are colored light gray with overlapping parts of two neighboring regions given in dark gray. For each region $P_{LM_-^n}$ its BCB boundary related to the condition $f_{LM_-^n}(z^-) = z^-$ is colored red and that related to the condition $f_{M_-LM_-^{n-1}}(-z^-) = -z^-$ is given in green. DFB boundaries are obviously defined by the same

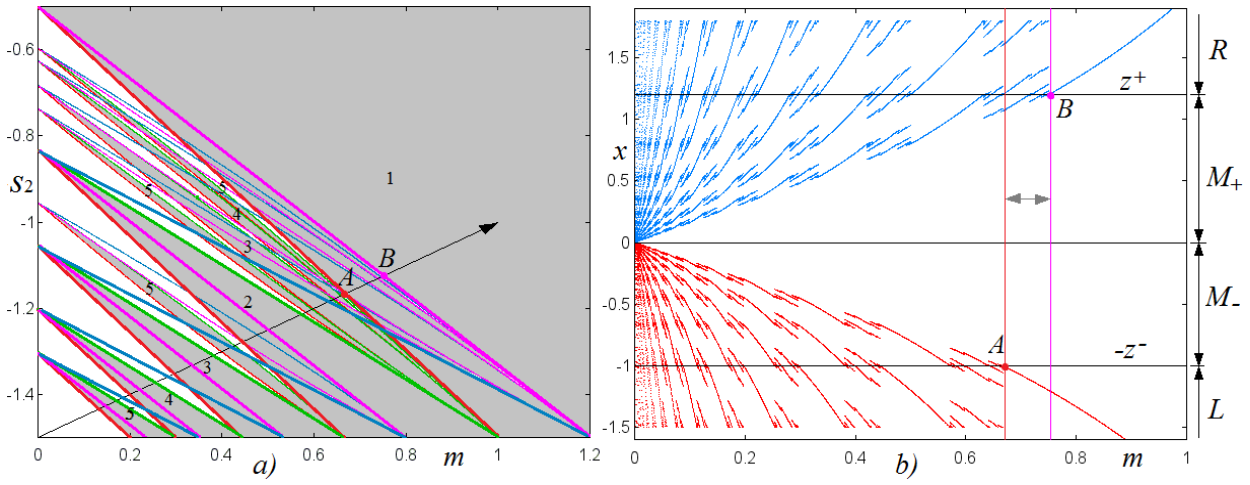

Figure 8: *a)* Boundaries of n-periodicity regions for $n = \overline{1,5}$, belonging to two period adding structures of map f given in (7) for $z^- = 1$ and $z^+ = 1.2$. Regions of the period adding structure associated with z^- are colored gray, and their boundaries are given in red and green, while the regions of the period adding structure related to z^+ are not colored, and their boundaries are given in blue and magenta. *b)* A 1D bifurcation diagram related to the parameter path indicated by the arrow in *a)*.

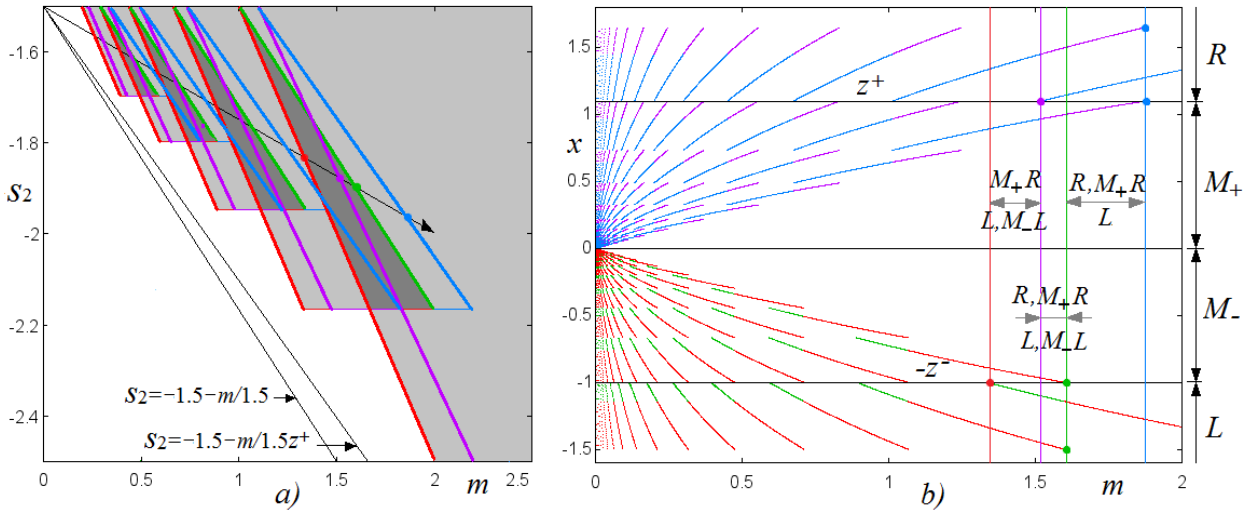

Figure 9: *a)* Boundaries of n-periodicity regions, $n = \overline{1,5}$, belonging to two period incrementing structures of map f given in (7) for $z^- = 1$ and $z^+ = 1.1$. Regions of the period incrementing structure associated with z^- are colored gray, and their boundaries are read and green, while regions of the structure related to z^+ are not colored, with boundaries given in blue and magenta. *b)* A 1D bifurcation diagram related to the parameter path indicated by the arrow in *a)*.

condition as in the symmetric case, that is, by the condition $(1+s_1+s_2)(1+s_1)^n=-1$. As for the period incrementing structure associated with discontinuity point $z^+=1.1$, in Fig. 9*a* only the boundaries of periodicity regions $P_{RM_+^n}$, $n=\overline{0,4}$, belonging to this structure, are colored: the BCB boundary of $P_{RM_+^n}$ related to the condition $f_{RM_+^n}(z^+)=z^+$ is colored magenta and that related to the condition $f_{M_+RM_+^{n-1}}(z^+)=z^+$ is given in blue. The overlapping part of $P_{RM_+^n}$ and $P_{RM_+^{n+1}}$ is associated with coexisting cycles RM_+^n and RM_+^{n+1}. The condition related to the DFB boundary of $P_{RM_+^n}$ is obviously the same as for region $P_{LM_-^n}$. Comparing these two period incrementing structures by means of 1D bifurcation diagram, it is easy to conclude which cycles may coexist, such as those indicated in Fig. 9*b*.

4.2 Distortion of the bifurcation structures in domains R_3 and R_4

Periodicity regions in domain R_3 are shown in Fig. 10 for $z^-=1$ and $z^+=1.1$. The 1D bifurcation diagram associated with the parameter path indicated in Fig. 10*a* is presented in Fig. 11*a*. This diagram provides evidence that there is still an even-period incrementing structure formed by regions $P_{LM_+^nRM_-^n}$, $n\geq 0$, with overlapping parts of the neighboring regions, which is qualitatively similar to that observed in the symmetric case (cf. Fig. 3*a*). However, Fig. 10 shows the appearance of new substructures.

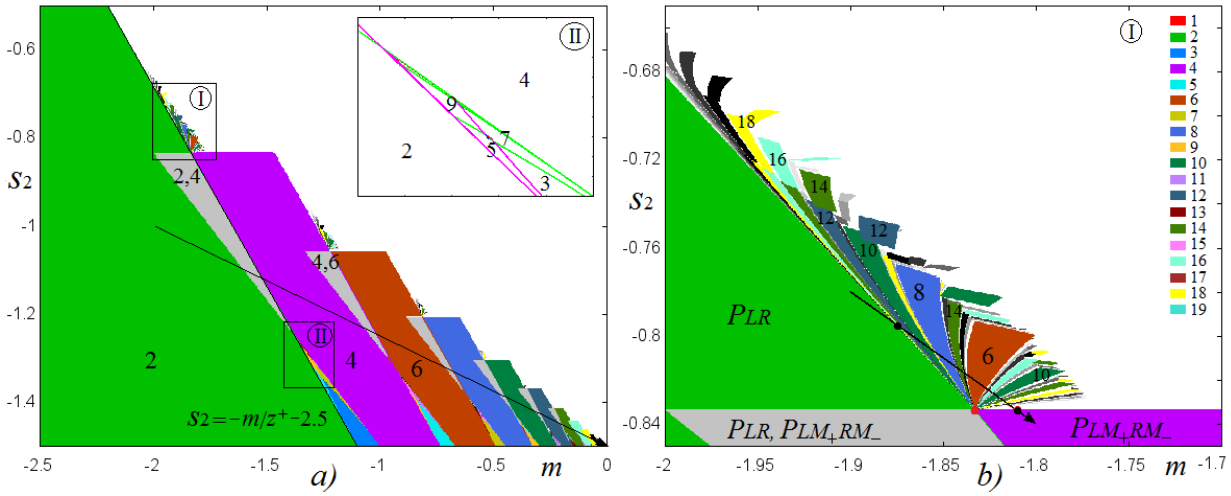

Figure 10: *a)* 2D bifurcation diagram in the (m,s_2)-parameter plane of map f given in (7) for $s_1=0.5$, $z^-=1$, $z^+=1.1$; *b)* An enlargement of the window indicated by I in *a)*.

Let us first comment on a substructure originating from an intersection point of the BCB and DB+1 boundaries of region $P_{LM_+^nRM_-^n}$, $n\geq 0$. As an example, in Fig. 10*b* we present an enlargement of the window indicated by I in Fig.

10*a*. It shows a period adding structure on the base of cycles LR and LM_+RM_-, which issues from the intersection point of the BCB boundary of P_{LR} given by $s_2 = -m/z^+ - (2 + s_1)$ and the DB+1 boundary of $P_{LM_+RM_-}$ given by $(1 + s_1 + s_2)(1 + s_1) = 1$. In Fig. 10 the BCB boundary is defined by $s_2 = -m/1.1 - 2.5$, the DB+1 boundary by $s_2 = -5/6$, and their intersection point is $(m, s_2) = (-11/6, -5/6)$ (shown in Fig. 10*b* by a red point). The period adding structure issuing from this point is illustrated in Fig. 12, which shows the 1D bifurcation diagram with an enlargement, related to the parameter path indicated in Fig. 10*b*. In order to see that the observed structure, is indeed a period adding structure first note that the DB+1 boundary of $P_{LM_+RM_-}$ also satisfies the condition of a BCB of cycle LM_+RM_-. In fact, for parameter values belonging to this DB+1 boundary, map f has four invariant intervals, each point of which is 4-periodic. Hence, the point $(m, s_2) = (-11/6, -5/6)$ can be seen as an intersection point of two BCB boundaries: one is related to cycle LR and the other to cycle LM_+RM_-. It is known that such a point, called the *big bang bifurcation point (or organizing center),* is an issue point of a period adding structure under certain additional conditions which are satisfied for the considered case (for details, see Gardini *et al.* (2014)). Similar structures are also described in Tramontana *et al.* (2012).

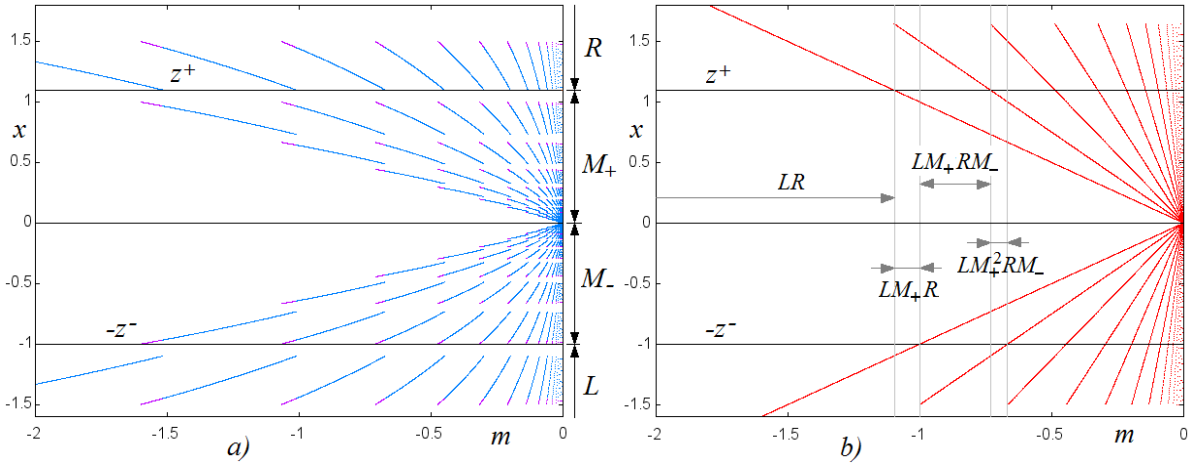

Figure 11: 1D bifurcation diagram of map f given in (7) for $s_1 = 0.5$, $z^- = 1$, $z^+ = 1.1$ and *a)* $s_2 = -0.25m - 1.5$, $-2 < m < 0$ (see the path indicated in Fig. 10*a*); *b)* $s_2 = -1.5$, $-2 < m < 0$.

One more difference with respect to the symmetric case $z^- = z^+$ concerns dynamics occurring for the parameter values belonging to the straight line $s_2 = -(1 + s_1)$, $m < 0$, associated with zero slope of the outermost branches of map f. For parameter values belonging to this line, one observes a period incrementing structure without overlapping,

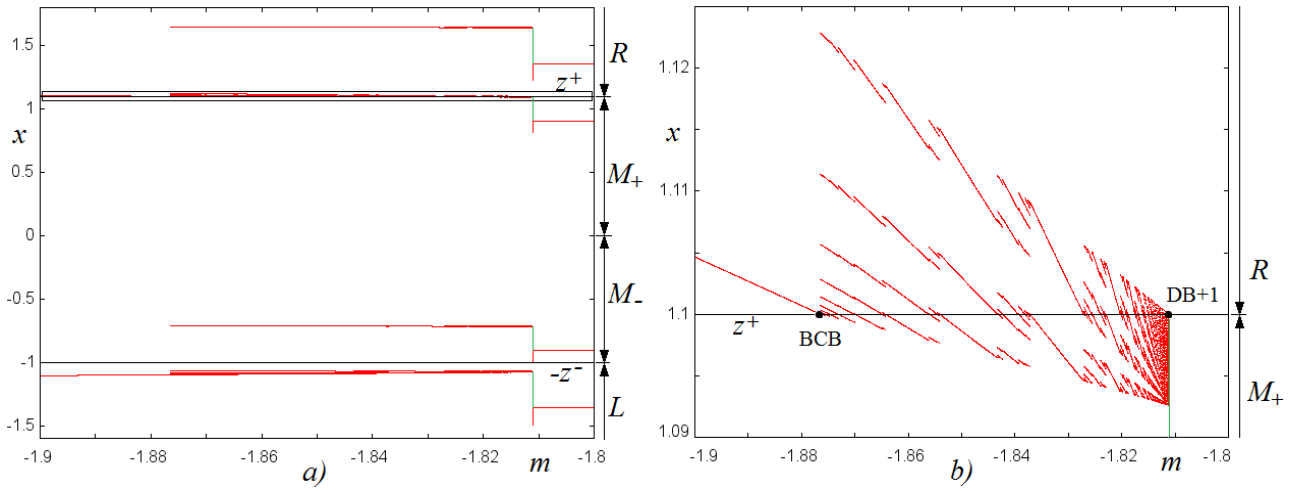

Figure 12: *a)* 1D bifurcation diagram of map f given in (7) for $z^- = 1$, $z^+ = 1.1$, $s_1 = 0.5$, $s_2 = -0.6m - 1.92$, $-1.9 < m < -1.8$ (see parameter path indicated in Fig. 10*b*); *b)* An enlargement of the window indicated in *a)*.

associated with superstable cycles of any period (not only even, as in the symmetric case). Such a period incrementing structure is formed by regions $P_{LM_+^nRM_-^n}$ and $P_{RM_-^nLM_+^{n+1}}$, $n \geq 0$, as illustrated in Fig. 11*b*. In fact, the 'additional' regions $P_{RM_-^nLM_+^{n+1}}$ extend to domain R_3 from domain R_4.

In the non-symmetric case in domain R_3 there are other substructures that are not observed in the symmetric case, located between any two neighboring regions $P_{LM_+^nRM_-^n}$ and $P_{LM_+^{n+1}RM_-^{n+1}}$, $n \geq 0$, such as the one visible in the window indicated by II in Fig. 10*a*. The BCB boundaries of the related periodicity regions are shown in the inset, where the periods of cycles associated with the biggest regions are also indicated. For a description of similar substructures, we refer to Tramontana *et al.* (2012c).

Finally, let us comment on how the period adding structure in domain R_4 is modified when the symmetry $z^- = z^+$ is broken. Recall that, in the symmetric case, the biggest periodicity regions visible in domain R_4 in Fig. 6*b* are regions $P_{LM_+^nRM_-^n}$, $P_{LM_+^nRM_-^{n+1}}$, $_{RM_-^nLM_+^{n+1}}$ for $n \geq 0$. In order to see how periodicity regions change if the value of z^+ increases, we show the boundaries of k-periodicity regions, $k = \overline{2,5}$, for $s_1 = 0.5$, $z^- = 1$ and $z^+ = 1.05$ in Fig. 13*a*, $z^+ = 1.1$ in Fig. 13*b*, $z^+ = 1.15$ in Fig. 14*a* and $z^+ = 1.2$ in Fig. 14*b*. Here, the regions colored gray are related to coexisting cycles, and for each periodicity region the BCB boundary related to the collision of a periodic point with discontinuity point $x = -z^-$ from the left/right is colored red/green, while the BCB boundary related to the collision of a periodic point with discontinuity point $x = z^+$ from the left/right is given in blue/magenta. One can see that there

are coexisting cycles not only of odd periods, as in the symmetric case, but also of even periods. Moreover, if the value of z^+ is incresed, the bistability regions associated with odd periods decrease while those with even periods increase.

In Fig. 15 we present a 1D bifurcation diagram for $z^+ = 1.1$, $m = -0.2$ and $-2.2 < s_2 < -1.8$ (see the parameter path shown in Fig. 13*b*). One can suggest that for $z^+ = z^- + \varepsilon$ for some sufficiently small $\varepsilon > 0$ each region $P_{LM_+^n RM_-^n}$, $n \geq 1$, includes region $P_{LM_+^{n+1} RM_-^{n-1}}$, and each region $P_{RM_-^n LM_+^{n+1}}$ includes regions $P_{LM_+^n RM_-^{n+1}}$. We leave the detailed investigation of this bifurcation structure for future work.

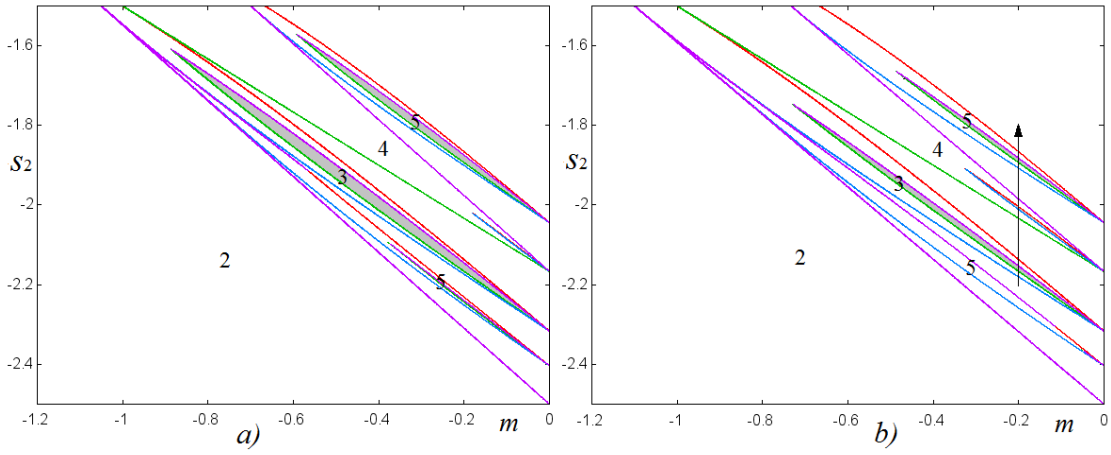

Figure 13: Boundaries of k-periodicity regions, $k = \overline{2,5}$, in the (m, s_2)-parameter plane of map f for $s_1 = 0.5$, $z^- = 1$ and $z^+ = 1.05$ in *a)*, $z^+ = 1.1$ in *b)*.

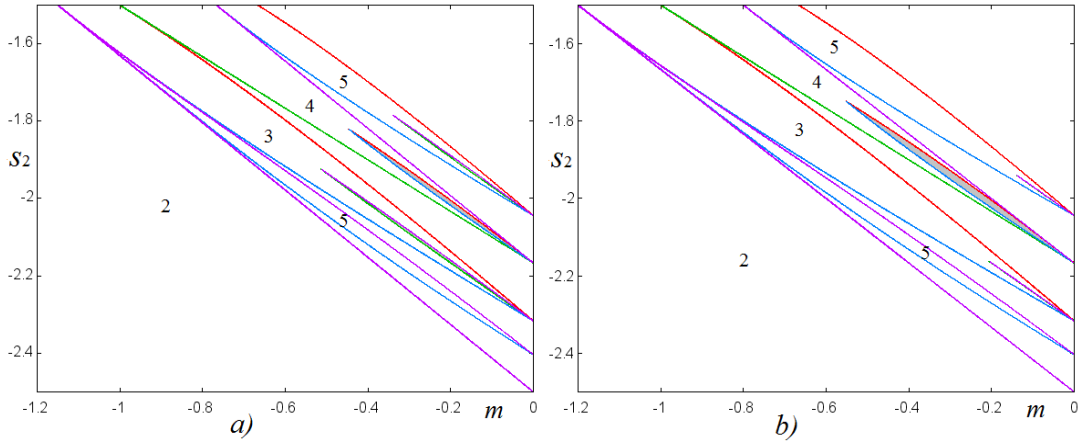

Figure 14: Boundaries of k-periodicity regions, $k = \overline{2,5}$, in the (m, s_2)-parameter plane of map f for $s_1 = 0.5$, $z^- = 1$ and $z^+ = 1.15$ in *a)*, $z^+ = 1.2$ in *b)*.

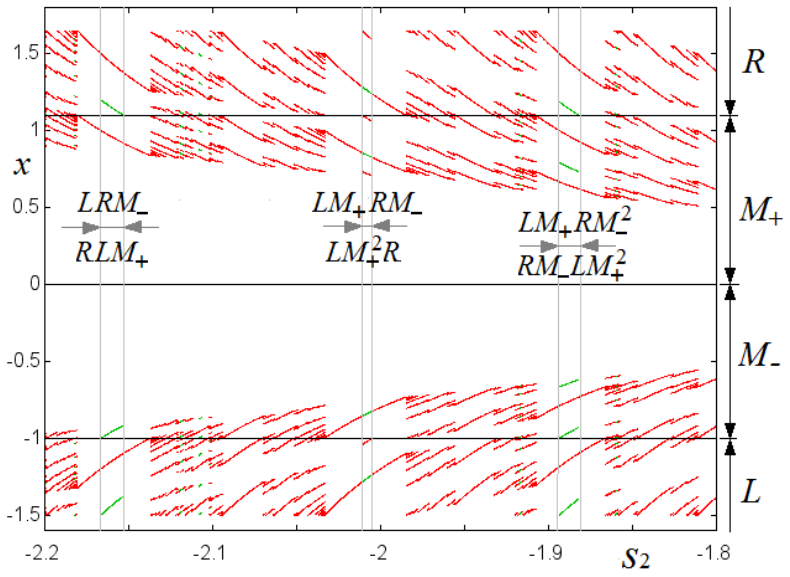

Figure 15: 1D bifurcation diagram of map f for $s_1 = 0.5$, $z^- = 1$, $z^+ = 1.1$, $m = -0.2$ and $-2.2 < s_2 < -1.8$ (the related parameter path is indicated in Fig. 13b by an arrow).

Only a few examples of the distortion of the bifurcation structures of domains R_3 and R_4 were discussed above. Examples of bifurcation structures of these domains for larger ε are presented in Fig.16. It is a challenging task to provide a complete description of the structures that may appear in these domains increasing ε, which will be left for future work.

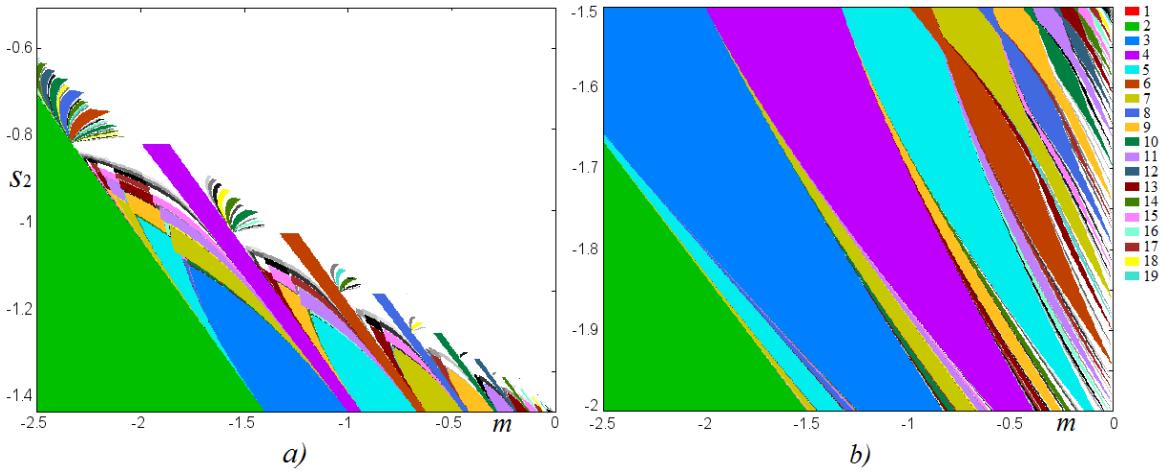

Figure 16: 2D bifurcation diagram in the (m, s_2)-parameter plane of map f given in (7) for *a)* $s_1 = 0.5$, $z^- = 1$, $z^+ = 1.4$; *b)* $s_1 = 0.5$, $z^- = 1$, $z^+ = 3$.

A few final economic remarks seem to be in order. To study the dynamics of our model, we neglect possible exogenous shocks. The analysis of regions R_1 to R_4 in this section reveals that a symmetry breaking of our map can greatly increase the complexity of the model's bifurcation structure. This is clearly witnessed by Figs. 10 to 15. Of course, the behavior of real market participants is random to some degree. Translated to our model, this means, in particular, that the model parameters will change over time and that the model dynamics will be subject to exogenous shocks. Consider, for instance, the situation depicted above the big bang bifurcation point in Fig. 10b. Apparently, even modest changes in parameters m and s_2 can turn the period-6 cycle, say, into a period-14 cycle, or into a period-2 cycle. Note that these cycles are associated with different volatilities and mispricings. In addition, exogenous shocks can push the dynamics from one attractor to another, making it even more difficult to predict the price dynamics. These observations suggest that our simple deterministic asset-pricing model, enriched by random components, can be useful for explaining the dynamics of real financial markets. While random forces are necessary to obtain a good fit of actual market dynamics, it is clear that the core of the dynamics will still depend on the model's (complex) bifurcation structure. For more details in this direction, see Tramontana *et al.* (2015).

5 Conclusions

The model studied in the present paper is defined by a 1D PWL map f with two discontinuity points. In Tramontana *et al.* (2013), the dynamics of this map was investigated for the special case $z^- = z^+$, implying that the map is symmetric with respect to the origin. This assumption considerably simplified the investigation of the bifurcation structures in the parameter space of the map, enabling four distinct bifurcation structures to be indentified: the period adding and period incrementing structures typical for maps with one discontinuity point, the even-period incrementing structure associated with two discontinuity points, and a particular period adding structure, which is also associated with two discontinuity points, the explicit description of which was left for future work. In the present paper, we consider this period adding structure in further detail. In particular, we obtain symbolic sequences of cycles of the first complexity level on the basis of which symbolic sequences of cycles of other complexity levels can be obtained. The main part of the paper is related to the symmetry breaking of the map. Accordingly, we investigate how the bifurcation structures existing in the symmetric case are modified when $z^+ = z^- + \varepsilon$ for some small $\varepsilon > 0$. We show that the standard period adding and period incrementing structures persist, being only quantitatively modified, while the bifurcation structures related to

two discontinuity points give rise to new substructures. In this way, the present paper contributes to the investigation of the overall bifurcation structure of the parameter space of a generic 1D PWL map with two discontinuity points, the complete description of which remains a challenging task with many unresolved problems.

However, we believe that our paper also makes a number of relevant economic contributions. Two of the most intriguing asset-pricing puzzles are associated with the observations that asset prices may persistently deviate from their fundamental values and that they are much more volatile than warranted by changes in their fundamental values. Apparently, these puzzles must have endogenous explanations. Our starting point is that the dynamics of financial markets is due largely to the behavior of its market participants. Indeed, the financial market model we present in this paper highlights interactions between chartists, fundamentalists and market makers, and is able to produce bubbles, crashes and excess volatility. We hope that our detailed analysis of the model's bifurcation structures – which reveal the existence and coexistence of cycles of different length, either located in the bull market, the bear market or even stretched over bull and bear markets – provide us with some novel insights to address these important puzzles.

Our paper may be extended in various directions. Let us briefly mention two of them. First, the dynamics of a stochastic version of our model can be studied. For example, one may assume that the reaction parameters of market participants and/or their market entry levels, (infrequently) change over time. The dynamics of such a model would then be the result of a combination of transients and cycles with different lengths and positions. In such a setup, a low volatility cycle may turn into a high volatility cycle, or a cycle located in the bull market may turn into a cycle involving bull and bear markets. Second, the 1D PWL map we study in our paper only contains the offset parameter m. By assuming that the price-independent demand of type 2 chartists and type 2 fundamentalists may differ in bull and bear markets, the map would have two different offset parameters, say m_1 and m_2. Of course, this would greatly complicate the analysis, which is why we started our analysis of the case with one offset parameter.

To conclude, we hope that our analysis is of use to other researchers studying 1D PWL maps. It is truly astonishing to see how rich the dynamics of a 1D PWL map can be. Obviously, such maps can be used to study many important economic and non-economic problems. In order to do so, however, more research is required in this exciting direction.

Acknowledgments

The authors express their gratitude to Laura Gardini for the valuable discussions they had with her. The work of I. Sushko and F. Westerhoff was performed under the auspices of COST Action IS1104 "The EU in the new complex

geography of economic systems: models, tools and policy evaluation". The work of V. Avrutin was supported by the European Community within the scope of the project "Multiple-discontinuity induced bifurcations in theory and applications" (Marie Curie Action of the 7th Framework Programme, Contract Agreement N. PIEF-GA-2011-300281).

References

Avrutin, V., Schanz, M. and Gardini, L. (2010): Calculation of bifurcation curves by map replacement. Int. J. Bifurcation and Chaos 20(10), 3105-3135.

Brock, W. and Hommes, C. (1998): Heterogeneous beliefs and routes to chaos in a simple asset pricing model. Journal of Economic Dynamics Control, 22, 1235-1274.

Chiarella, C. (1992): The dynamics of speculative behavior. Annals of Operations Research, 37, 101-123.

Chiarella, C., Dieci, R. and Gardini, L. (2005): The dynamic interaction of speculation and diversification. Applied Mathematical Finance, 12, 17-52.

Chiarella, C., Dieci, R. and He, X.-Z. (2007): Heterogeneous expectations and speculative behaviour in a dynamic multi-asset framework. Journal of Economic Behavior and Organization 62, 408-427.

Chiarella, C., Dieci, R. and He, X.-Z. (2009): Heterogeneity, market mechanisms, and asset price dynamics. In: Hens, T. and Schenk-Hoppé, K.R. (Eds.): Handbook of Financial Markets: Dynamics and Evolution. North-Holland, Amsterdam, 277-344.

Day, R. and Huang, W. (1990): Bulls, bears and market sheep. Journal of Economic Behavior and Organization, 14, 299-329.

Day, R. (1997): Complex dynamics, market mediation and stock price behavior. North American Actuarial Journal, 1, 6-21.

Gardini, L., Avrutin, V., and Sushko, I. (2014): Codimension-2 Border Collision Bifurcations in One-Dimensional Discontinuous Piecewise Smooth Maps. Int. J. of Bifurcation and Chaos 24(2) 1450024 (30 pages).

Gardini, L., Tramontana, F., Avrutin, V. and Schanz, M. (2010): Border Collision Bifurcations in 1D PWL map and Leonov's approach. Int. J. Bifurcation and Chaos, 20(10), 3085-3104.

Gardini, L. and Tramontana, F. (2010): Border Collision Bifurcations in 1D PWL map with one discontinuity and negative jump. Use of the first return map. Int. J. Bifurcation and Chaos, 20(11), 3529-3135.

Hommes, C. and Wagener, F. (2009): Complex evolutionary systems in behavioral finance. In: Hens, T. and

Schenk-Hoppé, K.R. (Eds.): Handbook of Financial Markets: Dynamics and Evolution. North-Holland, Amsterdam, 217-276.

Huang, W. and Day, R. (1993): Chaotically switching bear and bull markets: the derivation of stock price distributions from behavioral rules. In: Day, R. and Chen, P. (Eds.): Nonlinear Dynamics and Evolutionary Economics, Oxford University Press, Oxford, 169-182.

Huang, W., Zheng, H. and Chia, W.M. (2010): Financial crisis and interacting heterogeneous agents. Journal of Economic Dynamics and Control, 34, 1105-1122.

Huang, W. and Zheng, H. (2012): Financial crisis and regime-dependent dynamics. Journal of Economic Behavior and Organization, 82, 445-461.

Huang, W. and Chen, Z. (2014): Modelling regional linkage of financial markets. Journal of Economic Behavior and Organization, 99, 18-31.

Keener J.P. (1980): Chaotic behavior in piecewise continuous difference equations. Trans. Amer. Math. Soc. 261(2) 589-604.

Kirman, A. (1991): Epidemics of opinion and speculative bubbles in financial markets. In: Money and Financial Markets, edited by Mark Taylor, 354-368. Oxford: Blackwell.

Leonov, N.N. (1959): On a pointwise mapping of a line into itself. Radiofisica 2(6), 942-956.

Leonov, N.N. (1962): On a discontinuous pointwise mapping of a line into itself. Dokl. Acad. Nauk SSSR 143(5), 1038-1041.

Lux, T. and Marchesi, M. (1999): Scaling and criticality in a stochastic multi-agent model of a financial market. Nature 397, 498-500.

Lux, T. (2009): Stochastic behavioural asset-pricing models and the stylized facts. In: Hens, T. and Schenk-Hoppé, K.R. (Eds.): Handbook of Financial Markets: Dynamics and Evolution. North-Holland, Amsterdam, 161-216.

Sushko I., and Gardini L. (2010): Degenerate Bifurcations and Border Collisions in Piecewise Smooth 1D and 2D Maps. International Journal of Bifurcation & Chaos, 20(7) 2045-2070.

Tramontana, F., Gardini, L., Dieci, R. and Westerhoff, F. (2009): The emergence of 'bull and bear' dynamics in a nonlinear 3d model of interacting markets. Discrete Dynamics in Nature and Society, Vol. 2009, Article ID 310471, 30 pages.

Tramontana, F., Westerhoff, F. and Gardini, L. (2010): On the complicated price dynamics of a simple one-dimensional discontinuous financial market model with heterogeneous interacting traders. Journal of Economic Behavior and Organization, 74, 187-205.

Tramontana, F., Gardini L., Avrutin V. and Schanz M. (2012): Period Adding in Piecewise Linear Maps with Two Discontinuities. International Journal of Bifurcation & Chaos, 22(3) (2012) 1250068 (1-30).

Tramontana, F., Westerhoff, F., Gardini, L. (2013). The bull and bear market model of Huang and Day: Some extensions and new results. Journal of Economic Dynamics & Control 37, 2351-2370.

Tramontana, F., Westerhoff, F. and Gardini, L. (2015): A simple financial market model with chartists and fundamentalists: market entry levels and discontinuities. Mathematics and Computers in Simulation, Vol. 108, 16-40.

Tramontana, F., Westerhoff, F. and Gardini, L. (2014): One-dimensional maps with two discontinuity points and three linear branches: mathematical lessons for understanding the dynamics of financial markets. Decisions in Econonomics and Finance, 37, 27-51.

Westerhoff, F. (2004): Multiasset market dynamics. Macroeconomic Dynamics 8, 596-616.

Westerhoff, F. (2009): Exchange rate dynamics: a nonlinear survey. In: Rosser, J.B., Jr. (Ed): Handbook of Research on Complexity. Edward Elgar, Cheltenham, 287-325.